Kern, S., M. Brath, R. Fontes, M. Gade, K.-W. Gurgel, L. Kaleschke, T. Schlick, G. Spreen, S. Schulz, A. Winderlich, and D. Stammer (2009), "Multi^{3}Scat - A helicopter-based Scatterometer for Snow Cover and Sea Ice Investigations", *IEEE Geosci. Remote Sens. Lett.*, 6(4), 703-707, doi:10.1109/LGRS.2009.2023823.

Multi^{3}Scat—A Helicopter-Based Scatterometer for Snow-Cover and Sea-Ice Investigations

Stefan Kern, Manfred Brath, Rene Fontes, Martin Gade, Klaus-Werner Gurgel, Lars Kaleschke, Gunnar Spreen, Steffen Schulz, Andreas Winderlich, and Detlef Stammer

***Abstract*—A helicopter-based Doppler scatterometer (Multi^{3}Scat) is described. It allows simultaneous measurements of the surface radar backscatter at five different frequencies at co- and cross-polarization at incidence angles of 20°–65° from an altitude of 30–300 m. Video and infrared (IR) cameras simultaneously sense the surface in the scatterometers' footprint. The Multi^{3}Scat is calibrated using measurements carried out over corner reflectors. The stability of the Multi^{3}Scat's signal is found to be, on average, better than 0.5 dB. Typical signal-to-noise-ratio values for sigma-0 range between 10 and 20 dB for cross-polarization and between 15 and 25 dB for copolarization over snow and ice surfaces. The potential of the Multi^{3}Scat to acquire multifrequency multipolarization radar backscatter data and coincident video and IR temperature observations at different incidence angles over remote terrain such as the Arctic Ocean or the Alps is demonstrated.**

***Index Terms*—Infrared (IR) imaging, radar cross section, radar measurements, sea ice, snow.**

I. Introduction

ACCURATE knowledge of the distribution and thickness of thin ice is mandatory to quantify the wintertime ocean–atmosphere heat exchange in polar regions. Different single-frequency approaches to obtain the thickness of thin ice exist, which are mainly based on airborne synthetic aperture radar (SAR) data at C- [1] or X-band [2]. However, the maximum ice thickness which can be retrieved spans over one order of magnitude, 10–100 cm, and is thus apparently uncertain. This uncertainty could be explained with the highly variable physical properties of thin ice depending on its growth history, which determines its surface roughness, salinity, and temperature. This variability could cause ambiguous radar backscattering intensity changes with increasing ice thickness. Adding a second frequency [3] or using fully polarimetric data [4] could reduce effects caused by these ambiguous intensity changes on the retrieval of the thickness of thin ice. The optimal approach for this might involve a not yet considered combination of frequencies, polarizations, and incidence angles.

Accurate knowledge of the variability of snow accumulation and depletion is an asset for determining the onset of snowmelt runoff. The mapping of the required snow depth or snow water equivalent (SWE) is merely based on spaceborne microwave radiometry [5]. These products suffer from the coarse spatial resolution of a few tens of kilometers and the limited maximum snow depth to be retrieved. Using an active instead of a passive satellite microwave sensor would help to mitigate these shortcomings as has been demonstrated by [6], particularly when combining X- and Ku-band data [7]. Such a sensor, a dual-frequency SAR, called CoReH$_2$O, operating at X- and Ku-bands, is currently planned by the European Space Agency [8].

This letter introduces a scatterometer capable of obtaining surface-radar-backscatter data simultaneously at five different frequencies, four polarization combinations, and various incidence angles. Data obtained with this sensor could help to find the optimal approach needed to unambiguously identify thin ice and retrieve its thickness based on active microwave data. Its data could aid in the evaluation of CoReH$_2$O data and in the development of SWE retrieval algorithms based on its data. We describe the scatterometer, data processing, and quality and give examples of data obtained during two different campaigns.

TABLE I
Frequencies, Wavelengths, and Antenna Beamwidths of the Multi^{3}Scat

Frequency Band	L	S	C	X	Ku
Frequency [GHz]	1.0	2.4	5.3	10.0	15.0
Wavelength [cm]	30.0	12.5	5.7	3.0	2.0
Antenna Beam width (2-Way; 3dB) [°]	17.2	7.2	3.3	1.7	1.2

II. Multi^{3}Scat Instrument

The Multi^{3}Scat (Multi-cubed-Scat; Multi^3 stands for multipurpose, multifrequency, and multipolarization) sensor is a monostatic Doppler scatterometer with direct frequency conversion developed and built at the Institute of Oceanography, University of Hamburg (Table I and Fig. 1). Previous versions of this instrument were successfully used during campaigns in the North Sea [9] and the Arctic [10].

The system comprises a microwave unit, a control unit, a Direct Digital Synthesizer (DDS) module, and a data storage unit [Fig. 1(a)]. The radar signals are generated in the microwave unit in five identically designed separate modules (one per frequency; Fig. 1(b) shows the Ku-band module) using two phased-locked oscillators (PLOs), a transmitter and a receiver

Manuscript received October 29, 2008; revised March 13, 2009 and April 23, 2009. First published July 21, 2009; current version published October 14, 2009. This work was supported in part by the German Science Foundation under Program Sonderforschungsbereich SFB 512, by the European Space Agency under Contract 21146-07-NL-FF, and by the University of Hamburg under "Innovationsfond."

The authors are with the Centre for Marine and Atmospheric Sciences (ZMAW), Institute of Oceanography, University of Hamburg, 20146 Hamburg, Germany (e-mail: stefan.kern@zmaw.de; manfred.brath@zmaw.de; rene.fontes@zmaw.de; gade@ifm.uni-hamburg.de; klaus-werner.gurgel@zmaw.de; lars.kaleschke@zmaw.de; gunnar.spreen@jpl.nasa.gov; steffen.schulz@zmaw.de; andreas.winderlich@zmaw.de; detlef.stammer@zmaw.de).

Color versions of one or more of the figures in this paper are available online at http://ieeexplore.ieee.org.

Digital Object Identifier 10.1109/LGRS.2009.2023823

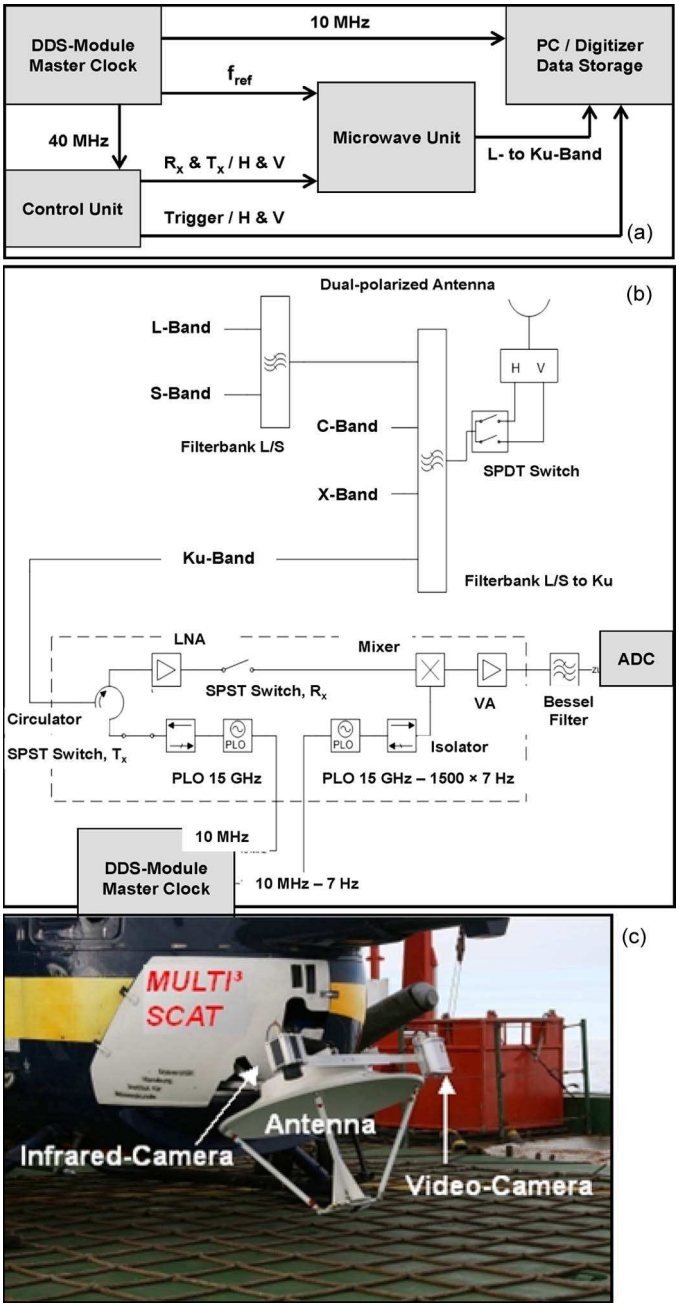

Fig. 1. Overview of components of the Multi^{3}Scat. See text for further details. Note that the frequency and factor given (15 GHz and 1500) are for Ku-band.

PLO, which upconvert two 10-MHz signals offset by 7 Hz, received by the DDS. The resulting frequency offset is 672, 1680, 3556, 6706, and 10 080 Hz at the L-, S-, C-, X-, and Ku-bands, respectively [Fig. 2: intermediate frequency (IF) peak in the spectral power density (SPD) plot]. Only the signal of the transmitter PLO is transmitted.

Microwave switches are triggered by the control unit and switch between transmission and reception. For each frequency band, the signal of the transmitter PLO is transmitted via the circulator of this module into a filter bank, where the signals of all bands are coupled [Fig. 1(b)]. The signal is subsequently fed into a broadband parabolic dish antenna via a dual-polarization broadband feed after decomposition into horizontal (H) or vertical (V) polarization using a switch [Fig. 1(b)].

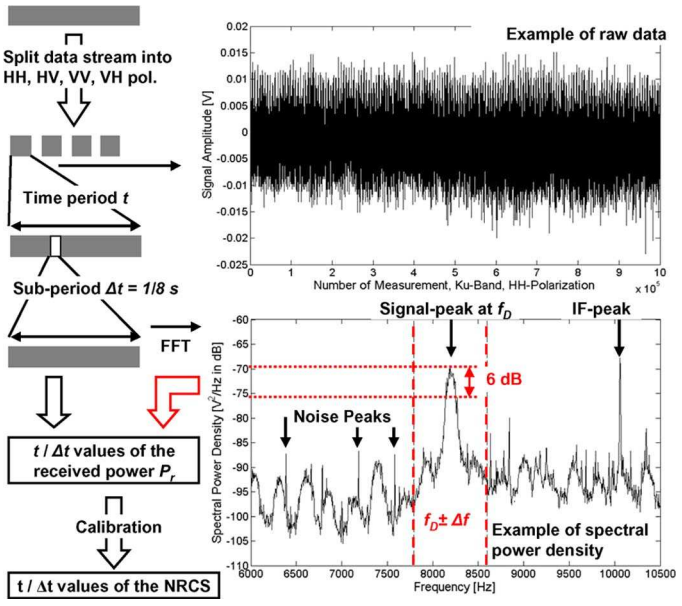

Fig. 2. Scheme of the radar data processing. See text for a detailed description.

This switch realizes the four polarization combinations by first transmitting and receiving at H-polarization (HH), then transmitting at H-polarization and receiving at V-polarization (HV), and then, accordingly, VV- and VH-polarization. One cycle through these combinations takes $1/PRF$ ($PRF =$ pulse repetition frequency) seconds.

The received signal is decoupled into the five frequencies via the filter bank and is fed into each separate module via the circulator of this module. It is amplified by a narrowband low-noise amplifier and then mixed with the signal of the receiver PLO. The resulting low-frequency signal is again amplified and filtered with a sixth-order low-pass Bessel filter with a 2-MHz cutoff frequency. Then, it is sampled at 10 MHz in a fixed-length reception window (1.3 μs), averaged over 12 samples, and saved.

The maximum PRF covering one full cycle of the transmission and reception of the signal at the four polarization combinations is 117.6 kHz. The minimum length of the transmitted pulse (for each polarization combination) is 0.5 μs. The pulselength can be changed to achieve a maximum overlap of the received filtered signal and the reception window for different flight altitudes. Typical values of pulselength and PRF during HeliSnow 2007/08 (ARKXXII/2) are 2.9 μs and 55.6 kHz (1.4 μs and 82.6 kHz); the values are larger for HeliSnow 2007/08 because of the larger flight altitude.

The components of the Multi^{3}Scat are mounted in an aluminum frame, which fits into a Messerschmitt–Bölkow–Blohm BO-105 helicopter. A lever at the end of the frame carries the antenna and video and infrared (IR) cameras, all looking into the same direction [Fig. 1(c)]. This lever enables us to change the surface incidence angle between 20° and 65° on flight. A gyro measures the helicopter's pitch and roll angle, which typically took values of about 2° and less than 2° during measurement conditions, respectively. The flight altitude is measured by the helicopter's radar altimeter. Two GPS receivers complement the system. The Multi^{3}Scat is operated via a graphical user interface.

The IR camera (VarioCAM Hr 384 M, JENOPTIK) uses a microbolometer focal plane array. The temperature resolution is about 0.1 K for a detector array of 384 $\times$ 288 pixels. The spectral range is 7.5–14 μm. The accuracy of the measured IR temperature is 1.5 K (or $\pm 2\%$ of the IR temperature) for -40 °C to 120 °C. It is equipped with a 50-mm telephoto lens with a viewing angle of $15^\circ \times 12^\circ$. The video camera (VC-Z22-48012, VC Germany) uses a 1/4″ Sony Super hole-accumulation diode charge-coupled device chip (480TVL) to obtain color video images with 752 $\times$ 582 pixels. The spectral range is 380–800 nm. It uses a standard lens with a viewing angle of $30^\circ \times 24^\circ$. Both cameras are heated and can be operated at outside temperatures as low as -20 °C (IR) or -25 °C (video). Their data are streamed at 10 Hz onto the operator's notebook hard disk.

III. Data Processing and Quality

Fig. 2 shows a schematic overview about the Multi^{3}Scat data processing. Each data file contains data of t seconds of flight time. These data are first split into the four polarization combinations (see Fig. 2, upper right, for an example of a part of Ku-band HH-polarized raw data) and further into 1/8-s-long subperiods. For each subperiod, an FFT is run to obtain the SPD (Fig. 2). This spectrum shows the IF, the signal peak at the Doppler frequency f_D, and the noise peaks, which are subsequently filtered out. The received power P_r is obtained as the integral of the topmost 6 dB of the SPD of the signal peak in a frequency interval of 2 Δf centered around f_D (Fig. 2, red lines and letters).

For the calibration, Multi^{3}Scat flights are carried out repeatedly over a chain of five quasi-trihedal (quadratic base plate) and two trihedal corner reflectors (CRs) put on a runway made of concrete. Flight altitudes and speeds are the same as during the campaigns; the incidence angle was 45°. Coincident video imagery aids to identify those CR overpasses where at least one CR is hit optimally. Copolarized Multi^{3}Scat data of these (eight) overpasses are taken to calculate the calibration factors E separately for each frequency band. The normalized radar cross section (σ^0) is subsequently computed using (derived from [11])

$$\sigma^0 = EP_r = \frac{\sigma^0_{\mathrm{CR}} R^4}{P_{\mathrm{CR}} R^4_{\mathrm{CR}} A} P_r.$$

R and R_{CR} are the distances to the surface and the CRs (calculated from the incidence angle and the helicopter's attitude data), A is the footprint size at the surface (calculated using R and the antenna beamwidths), P_{CR} is the power received from the CRs (it is assumed that the background signal can be neglected for the used frequencies at 45° incidence angle), and σ^0_{CR} is the radar cross section of the CRs. Cross-polarized data are calibrated using the average of E obtained for both copolarizations (difference is, on average, smaller than 0.2 dB).

Table II exemplifies the average overall signal-to-noise ratio (SNR) and the average minimum SNR (average of those SNR values, which are smaller than the mean SNR minus two standard deviations) for σ^0 obtained with the Multi^{3}Scat at C-, X-, and Ku-bands during HeliSnow2007-08 at Leutasch, January 14, 2008 (values for L- and S-bands are similar to those shown for C-band). Evidently, the SNR of the copolarized σ^0 values is fine but could hit the noise floor at cross-polarization, particularly at shallow incidence angles and/or at X-band. The noise floor itself has a standard deviation of 1.5–2.0 dB at X- and Ku-bands and 0.5–1.5 dB otherwise.

TABLE II
(BOLD) AVERAGE SNR AND AVERAGE MINIMUM SNR (SEE TEXT) FOR σ^0 VALUES OBTAINED AT C-, X-, AND KU-BANDS AT LEUTASCH JANUARY 14, 2008. ALL VALUES ARE GIVEN IN DECIBELS

f[GHz]	5.3	10.0	15.0
Co-Pol. [dB]	**19.5** / 10.7±1.2	**12.2** / 4.5±1.2	**13.9** / 7.2±1.2
	23.8 / 18.0±0.9	**16.2** / 8.9±1.4	**18.6** / 12.0±1.1
Cross-Pol.[dB]	**10.8** / --	**5.3** / --	**11.3** / 3.6±1.1
	14.7 / 4.8±1.0	**8.0** / --	**16.0** / 9.3±1.2

IV. Results

A. Multi^{3}Scat Observations During Helisnow2007–08

The campaign HeliSnow2007–08 took place in the Alps close to Innsbruck, Austria. The aim was to obtain radar backscatter observations of the snowpack for different typical snow properties. Multi^{3}Scat measurement flights were carried out at same heading, speed (about 30 m/s), and altitude (about 180 m) along flight lines (length: 2–7 km) at five different locations on December 14–15, 2007 and January 14, 2008. At each location, four overpasses (two with 25° and two with 45° incidence angle) were completed. *In situ* measurements of snow physical properties complement these data [12]. Fig. 3 shows an example of the data (Multi^{3}Scat, video and IR cameras) obtained at Leutasch on January 14, 2008. The snow depth (five snow pits distributed along the flight line) was 45 $\pm$ 4 cm, and the SWE was 128 $\pm$ 12 mm. The snowpack comprised coarse-grained (average grain size: 2 mm) snow in multiple (ice) layers with about 5 cm of new snow on top (T. Nagler, 2008, personal communication).

Table III summarizes the preliminary σ^0 values averaged over 10-s flight time (300 m) for meadows and a spruce forest at Leutasch, January 14, 2008. The standard deviation of these values is 1–2 dB. According to model studies, such an error would translate into an uncertainty in retrieved SWE of about 100 mm at X-band and 40 mm at Ku-band [8]. Note that the values shown in Table III are based on 1) a limited data set and 2) a preliminary data processing, which, at the time of writing, was optimized to identifying small leads in the sea-ice cover. The usage of a longer subperiod Δt to calculate P_r (see Fig. 2) would substantially reduce the standard deviation.

The σ^0 values obtained with the Multi^{3}Scat at C-band for spruce forests (Table III, 45°) agree within one standard deviation with observations carried out in Finland under similar conditions (Alasalmi *et al.* in [13]): -8 dB at HH-polarization and -14 dB at HV-polarization and an incidence angle of 50°. Values of σ^0 for snow-covered agricultural land are about 3–4 dB lower (Alasalmi *et al.* [13]) than our values for snow-covered meadows (Table III, 45°). This could be explained with a different soil surface roughness. Typical σ^0 values obtained for the forest canopy in Finland during summer are -8.5 dB at HH-polarization and -15 dB at HV-polarization at C- and X-band (Hallikainen *et al.* [13]). These values are quite similar

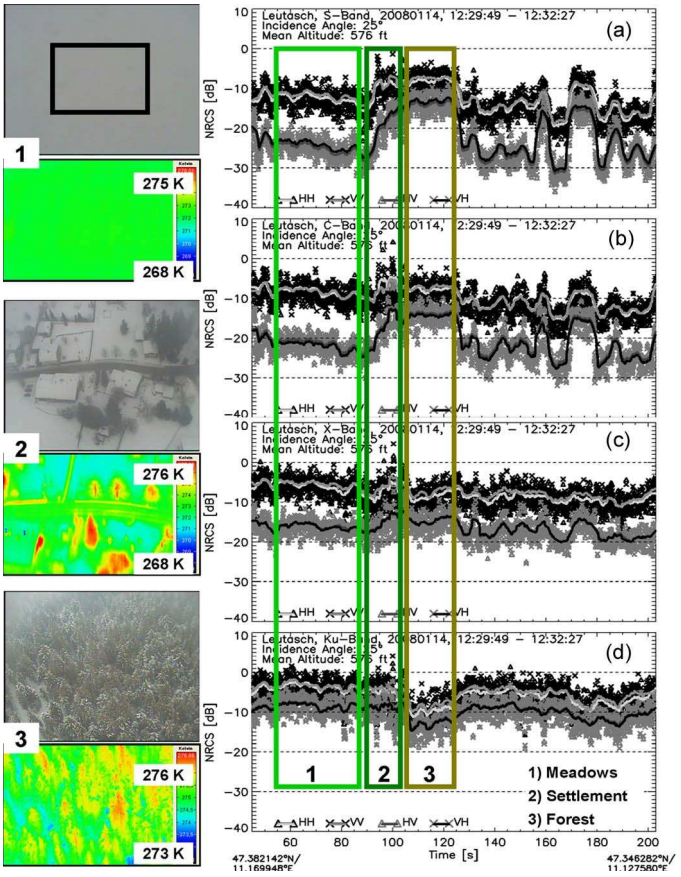

Fig. 3. Values of σ^0 obtained at Leutasch on January 14, 2008 (altitude: 180 m, incidence angle: 25°) for (a)–(d) S-, C-, X-, and Ku-bands. Black and gray symbols denote co- and cross-polarized σ^0 values at 1/8-s temporal resolution, respectively; thick lines show σ^0 values averaged over 100 m. Green boxes numbered 1–3 denote the specific surface areas for which examples of video and IR images are given. The box in the video image of image pair 1 marks the size and location of the IR image.

TABLE III
TYPICAL σ^0 VALUES (IN DECIBELS) OBTAINED AT (BOLD) HH- AND (ITALIC) HV-POLARIZATION FOR SNOW-COVERED MEADOWS AND FORESTS AT LEUTASCH, JANUARY 14, 2008 (SEE FIG. 3, FRAMES 1 AND 3). THE STANDARD DEVIATION IS ON THE ORDER OF 1–2 dB. VV-POLARIZATION VALUES ARE SIMILAR TO HH-POLARIZATION VALUES WITHIN THE GIVEN STANDARD DEVIATION

	25° - Meadows - 45°		25° - Forest - 45°	
S	**-12** / *-25*	**-17** / *-28*	**-8** / *-14*	**-9** / *-15*
C	**-8** / *-21*	**-14** / *-23*	**-7** / *-14*	**-9** / *-15*
X	**-5** / *-16*	**-9** / *-18*	**-7** / *-15*	**-9** / *-16*
Ku	**-3** / *-8*	**-6** / *-11*	**-8** / *-12*	**-10** / *-13*

to those reported by Alasalmi *et al.* [13] for C-band and agree also with our results.

B. Multi^{3}Scat Observations During ARKXXII/2

The expedition ARKXXII/2 of the German research icebreaker *Polarstern* into the Arctic Ocean took place from July 28 to October 7, 2007 [14]. The focus of the involved Multi^{3}Scat measurements was on improved melt-pond and thin-ice identification. About 24 measurement flights were completed. Ten of these occurred along tracks of which a subsection was marked on the ice prior to the overpass. The flights

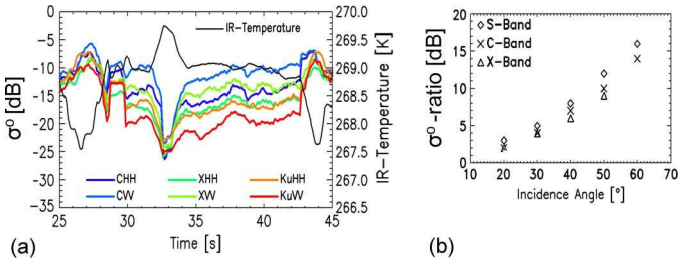

Fig. 4. (a) σ^0 values obtained with the Multi^{3}Scat at (blue) C-, (green) X-, and (red) Ku-bands at 35° incidence angle from an altitude of 30 m together with (black) coincident IR temperature observations during ARKXXII/2, September 16, 2007. See text for more details. (b) Peak copolarization ratio at S-, C-, and X-bands as a function of the incidence angle for a lead covered with 2-cm-thick dark nilas observed with the Multi^{3}Scat on August 24.

TABLE IV
LINEAR CORRELATION COEFFICIENT BETWEEN IR TEMPERATURE AND (BOLD) σ^0 VALUES FOR C-, X-, AND KU-BANDS FOR SEPTEMBER 16, 2007, TOGETHER WITH TYPICAL VALUES OF σ^0 (IN DECIBELS) AT HH- AND VV-POLARIZATION FOR INCIDENCE ANGLES OF 35° AND 50° FOR (NORMAL) LIGHT NILAS/GRAY ICE AND (ITALIC) BROKEN ROUGH FIRST-/SECOND-YEAR ICE. VALUES (IN DECIBELS) GIVEN IN COLUMNS ON35 AND ON50 ARE FOR HH-POLARIZATION AT 35° AND 50° TAKEN BY ONSTOTT IN [15]

	HH35	ON35	VV35	HH50	ON50	VV50
C	**-0.83**		**-0.75**	**-0.83**		**-0.51**
	-14.5±2.7		-11.0±1.2	-15.9±2.2		-10.4±1.3
	-8.2±1.6	*-15*	*-7.4±1.9*	*-8.8±1.9*	*-16*	*-8.1±1.8*
X	**-0.87**		**-0.82**	**-0.87**		**-0.86**
	-16.6±2.0		-14.3 ± 1.3	-18.7±3.3		-16.0±1.4
	-10.0±1.9	*-9*	*-9.3 ± 1.5*	*-9.7±2.2*	*-9*	*-8.9±2.0*
Ku	**-0.93**		**-0.91**	**-0.90**		**-0.90**
	-18.1±3.7		-20.1±4.7	-19.7±10.8		-22.5±10.0
	-7.3±1.4	*-6*	*-9.4±1.3*	*-6.6±2.1*	*-6*	*-8.6±2.0*

were carried out using five different incidence angles (20–60°) with the same heading, speed (about 40 m/s), and altitude (30 or 60 m). From ice cores drilled along the subsections and scaled digital photography, sea-ice physical properties were obtained. More measurement flights took place as long-distance underflights of a scheduled satellite radar image or as short-distance flights over specifically selected ice areas.

Fig. 4(a) shows a 20-s (700-m)-long subset of Multi^{3}Scat data and IR-temperatures (T_{IR}), which have been averaged over the size of the radar footprint on the ground, for a measurement flight on September 16, 2007. A patch of light nilas/gray ice (thickness: 10–15 cm) embedded in a matrix of broken thicker ice floes was overpassed two times [altitude: 30 m, speed: 35 m/s, incidence angles: 35° and 50° (not shown)]. Data are smoothed with a 1-s-long (35 m) moving average. Cross-polarized data are not shown because of a too low SNR over dark nilas.

The σ^0 values are inversely correlated with the IR temperatures, particularly at HH-polarization (Table IV). The lowest σ^0 values [between -23 and -27 dB, Fig. 4(a)] are observed for dark nilas ($T_{\mathrm{IR}} > 269.5$ K, approximate thickness: 3 cm). These σ^0 values agree with backscatter measurements carried out at C- and X-bands over thin ice grown in an outdoor tank (Winebrenner *et al.* [15]). The highest σ^0 values [Fig. 4(a) and Table IV] are observed for the broken rough first-year ice at the transition to second-year ice ($T_{\mathrm{IR}} < 268.0$ K). Such ice

has already radar backscattering properties similar to those of multiyear ice (Onstott [15]). Because it is broken and rough, its σ^0 values at C-band are larger than those typically observed over multiyear ice under freezing conditions (Table IV, ON35 and ON50). The σ^0 values observed for light nilas/gray ice [Fig. 4(a), T_{IR} around 269.0 K] depend strongly on the frequency and polarization combination (Table IV). Compared with laboratory-based radar backscatter measurements over light nilas/gray ice, the σ^0 values presented here are too high: C-band VV-polarization, 35°: -11 dB versus -22 dB (Swift *et al.* [15]). This could be explained 1) by differences in the environmental conditions and 2) by the high surface temperature encountered during our measurements (-2 °C), which could cause σ^0 values higher by 3–6 dB compared with those of cold conditions [15].

The copolarization ratio (CPR), i.e., σ^0 at VV-polarization divided by σ^0 at HH-polarization increases with increasing incidence angle. This is visible in Table IV for C-band (35°: 3.5 dB; 50°: 5.5 dB) and is shown in Fig. 4(b) in agreement with that of Onstott [15]. The larger CPR shown in Fig. 4(b) at C-band compared with the one given in Table IV is caused by the smaller ice thickness: August 24: 2 cm and September 16: 10–15 cm.

One possible application of this multifrequency data would be an improved two-step thin-ice thickness retrieval algorithm. First, the larger σ^0 difference between thin and thick ice at Ku-band compared with that of C-band could yield a more accurate identification of thin ice. Subsequently, the CPR at C-band (or a lower frequency [10]) could be used to obtain the ice thickness.

V. Summary

The helicopter-based Doppler scatterometer Multi^{3}Scat has been described. It can be used for radar backscatter measurements of the surface at five different frequencies (L- to Ku-band), both co- and cross-polarization combinations, and incidence angles of 20°–65° from altitudes of 30–300 m. Video and IR cameras simultaneously sense the surface within the scatterometers' footprint. The data processing is described. The Multi^{3}Scat is calibrated with radar backscatter measurements over CRs. The stability of the emitted radar signal is found to vary by 0.25 dB (L- to X-band) and 0.8 dB (Ku-band). Typical SNR values for σ^0 range between 10 and 20 dB (15 and 25 dB) for cross (co-)-polarization over snow and sea ice; they reduce by about 10 dB over new level sea ice.

Values of σ^0 obtained with the Multi^{3}Scat during the campaign HeliSnow2007–08 in the Alps on January 14, 2008 agree with results from previous studies under similar environmental conditions. Changes in σ^0 can be quantified for different frequencies at a glance and can be associated unambiguously to the respective surface properties by the combination with coincident video and IR imagery. The latter could particularly help in interpreting Multi^{3}Scat data by providing surface temperature estimates.

Values of σ^0 obtained with the Multi^{3}Scat during the expedition ARKXXII/2 of the R/V Polarstern into the Arctic Ocean in the fall of 2007 are discussed in relation to results of previous studies. The potential of the Multi^{3}Scat to identify changes in σ^0 as a function of incidence angle and polarization combination over similar surface types similarly at C-, X- and Ku-bands is demonstrated. It is shown that the magnitude of the copolarization ratio observed at C-, X-, and Ku-bands over light nilas/gray ice with 10–15-cm thickness increases with incidence angle but shows an opposite sign at Ku-band.

Acknowledgment

The authors would like to thank HeliService International, GmbH, Germany, Tyrolean and the airport, Innsbruck, Austria, the R/V Polarstern crew, the logistics of the Alfred Wegener Institute, and the scientific crews during ARKXXII/2 and HeliSnow 2007/08 for their support and the two anonymous reviewers whose comments helped to improve this letter substantially.

References

[1] R. Kwok, S. V. Nghiem, S. H. Yueh, and D. D. Huyngh, "Retrieval of thin ice thickness from multifrequency polarimetric SAR data," *Remote Sens. Environ.*, vol. 51, no. 3, pp. 361–374, Mar. 1995.

[2] K. Nakamura, H. Wakabayashi, K. Naoki, F. Nishio, T. Moriyama, and S. Uratsuka, "Observation of sea-ice thickness in the sea of Okhotsk by using dual-frequency and fully polarimetric airborne SAR (Pi-SAR) data," *IEEE Trans. Geosci. Remote Sens.*, vol. 43, no. 11, pp. 2460–2469, Nov. 2005.

[3] E. Rignot and M. R. Drinkwater, "Winter sea-ice mapping from multiparameter synthetic-aperture radar data," *J. Glaciol.*, vol. 40, no. 134, pp. 31–45, 1994.

[4] W. Dierking, H. Skriver, and P. Gudmandsen, "On the improvement of sea ice classification by means of radar polarimetry," in *Remote Sensing in Transition*, R. Goossens, Ed. Rotterdam, The Netherlands: Millpress, 2003, pp. 203–209.

[5] R. E. J. Kelly and A. T. C. Chang, "Development of a passive microwave global snow depth retrieval algorithm for Special Sensor Microwave/Imager (SSM/I) and Advanced Microwave Scanning Radiometer-EOS (AMSR-E) data," *Radio Sci.*, vol. 38, no. 4, p. 8076, 2003, DOI:10.1029/2002RS002648.

[6] S. V. Nghiem and W.-Y. Tsai, "Global snow cover monitoring with spaceborne Ku-band scatterometer," *IEEE Trans. Geosci. Remote Sens.*, vol. 39, no. 10, pp. 2118–2134, Oct. 2001.

[7] D. Floricioiu and H. Rott, "Seasonal and short-term variability of multifrequency, polarimetric radar backscatter of alpine terrain from SIR-C/X-SAR and AIRSAR data," *IEEE Trans. Geosci. Remote Sens.*, vol. 39, no. 12, pp. 2634–2648, Dec. 2001.

[8] M. Kern, "Candidate earth explorer core mission: CoReH2o—Cold regions hydrology high-resolution observatory," ESA, Nordwijk, The Netherlands, p. 114, 2008.

[9] M. Gade, W. Alpers, H. Hühnerfuss, and V. Wismann, "On the reduction of the radar backscatter by oceanic surface films: Scatterometer measurements and their theoretical interpretation," *Remote Sens. Environ.*, vol. 66, no. 10, pp. 52–70, Oct. 1998.

[10] S. Kern, M. Gade, A. Pfaffling, and C. Haas, "Retrieval of thin-ice thickness using the L-band polarization ratio measured by the helicopter-borne scatterometer HELISCAT," *Ann. Glaciol.*, vol. 44, no. 1, pp. 275–280, 2006.

[11] L. J. Battan, *Radar Observations of the Atmosphere*, vol. 324. Chicago, IL: Univ. Chicago Press.

[12] H. Rott, T. Nagler, S. Kern, D. Stammer, H. Rebhan, and J. Shi, "Studies of multi-frequency polarimetric backscattering characteristics of snow cover and glacier measured in the HELISNOW-2008 campaign," in *Proc. IGARSS*, Boston, MA, Jul. 6–11, 2008.

[13] M. Beorgeaud, "Second international workshop on retrieval of bio- and geo-physical parameters from SAR data for land applications," ESA-ESTEC, Nordwijk, The Netherlands, p. 614, Oct. 21–23, 1998.

[14] U. Schauer, "The expedition ARKTIS-XXII/2 of the research vessel 'Polarstern' in 2007," in *Reports on Polar and Marine Research*, vol. 579. Bremerhaven, Germany: Alfred-Wegener Inst. Polar and Marine Res., 2008.

[15] F. D. Carsey, "Microwave remote sensing of sea ice," in *Geophysical Monograph*, vol. 68. Washington, DC: Amer. Geophys. Union, 1992.